# EFFECTS OF 3D-PRINTED HORSESHOES ON KINEMATIC HOOF-PARAMETERS AT TROT ON HARD SURFACE

_____

## MASTER THESIS VETERINARY MEDECINE

## UTRECHT UNIVERSITY

**AUTHOR:**

SOLVOR NYLAND MALMEI

5872995 S.N.MALMEI@STUDENTS.UU.NL


**SUPERVISORS:**

J.I.M. PARMENTIER MSC

DEPARTMENT OF CLINICAL SCIENCE, EQUINE DEPARTMENT

FACULTY OF VETERINARY MEDICINE

UTRECHT UNIVERSITY, THE NETHERLANDS


MARCH 2022

**Preface**

This thesis was conducted as part of the master's degree of Veterinary Medicine at Utrecht University, The Netherlands, Faculty of Veterinary Medicine, Department of Clinical Sciences, Equine Department.

The aim of the study was to investigate the effects of 3D-printed horseshoes on equine kinematics parameters using Internal Measurement Unit system. The data was obtained at Utrecht University at the department of Clinical Sciences. In addition to kinematic data, data regarding kinetics, as well as wear of the shoes and hoof growth and angles, were measured and collected. However, only the data concerning hoof kinematic parameters will be subject of this master thesis.

I would like to thank my supervisor Jeanne Parmentier for the incredible support and indispensable academic knowledge throughout the progress of this master thesis. Her supervision, time and effort have been essential during the process and the finalisation of this thesis.

I also wish to show my appreciation to Prof. Dr. Harold Brommer, and all the other people involved in this project of the Department of Clinical Sciences at Utrecht University, for giving me the opportunity to be part of this incredible interesting research project.

Last, but not least, I would like to thank my grandfather, em Prof. Dr. Med. Harald Nyland, for always encouraging learning and academic skills from an early age, and for giving me advice on the process of scientific research.

_____

Solvor Nyland Malmei

# List of abbreviations, figures, tables, and appendices

**Abbreviations:**

3D: Three-dimensional

GRF: Ground reaction force

IMU: Inertial measurement unit

Max (Parameter): Maximum signal value

Min (parameter): Minimum signal value

OMC: Optical motion capture

PeakNeg: Number of peaks on the negative side of the signal

PeakPos: Number of peaks on the positive side of the signal

UU: Utrecht University

**Figures:**

**Tables:**

**Appendices:**

# Abstract

**Background:** Proper and adequate shoeing is important to maintain and promote a functional foot. However, fitting a horseshoe can be challenging, especially in horses with hoof-related problems.

**Objectives**: The purpose of this study is to investigate the effects of tailor-made three-dimensional (3D)-printed horseshoes on equine hoof kinematic parameters in a controlled experimental setting, using quantitative gait-analysis system. We hypothesised that 3D-printed horseshoes would cause less vibrations and impact on hard surface.

**Methods:** Six rider-sound horses were shod with traditional steel shoes for two shoeing-cycles and one shoeing-cycle of 3D-printed horseshoes made of a thermoplastic elastomer, in a randomised order. Kinematic data was collected on a straight line at trot on hard surface, using hoof mounted inertial measurement units (IMU), including accelerometers (sampling frequency: 1000 Hz), one day after shoeing. A linear mixed effect model was used to determine the effect of shoeing-condition on the kinematic parameters extracted, with Horse as a random effect and Shoes type and Stride frequency as fixed effects.

**Results:** Among the extracted parameters, the ones significantly different were the lower Max acceleration values in the mediolateral ($-145.25$ m/s$^2$, p-value=0.049) and in dorsopalmar directions ($-263.24$ m/s$^2$, p-value=0.0001). The signals contained less energy in mediolateral and dorsopalmar directions ($-4673.63$ (m/s$^2$)$^2$, p-value = 0.0107 and $-6162.13$(m/s$^2$)$^2$, p-value=0.0149, respectively). The Peak-Positive and Peak-Negative counts were larger in dorsopalmar direction ($-1.58148$, p-value=0.01742 and $-1.56364$, p-value=0.01888 respectively). No significant differences were found in proximodistal direction.

**Conclusion:** These findings suggest that 3D-printed horseshoes decrease vibrations and have an impact absorbing effect on hard surface at trot.

**Keywords:** horse, horseshoes, 3D-print, kinematics, trot, hard surface, IMU, accelerometer

# Content

# I.  Introduction

Proper and adequate shoeing is important for horse's soundness, promotes a functional foot, prevent lameness, and influences a horse's performance. Variants of horseshoes are used to protect and prevent hooves from excessive wearing, the Celts being the first to use steel shoes nailed to the hoof 2000 years ago (Back and Clayton 2013). For centuries, horseshoes have been fitted to the hoof by a farrier based on tradition, empirical evidence, and personal experience (Weller et al. 2018; Eliashar 2007). Fitting a horseshoe can be challenging, especially in horses with hoof-related problems or orthopaedic deviations.

Recently, researchers and farriers from the Equine section of the Department of Clinical Sciences (DCS) at Utrecht University (UU) developed innovative 3D-printed horseshoes made of a synthetic plastic composition. These 3D-printed horseshoes are printed based on a 3D-scan of the hooves and are thereafter glued directly onto the hoof wall. This research project will investigate the effects of the 3D-printed horseshoes on equine locomotion parameters in a controlled experimental setting. Kinematic and kinetic studies were organised at Utrecht University, involving six horses over a total of three shoeing-cycles of seven weeks each, consisting of one shoeing-cycle with 3D-printed shoes, to be compared to two shoeing-cycles with traditional steel shoes.

The aim of this master thesis was to investigate the effects of tailor-made 3D horseshoes on kinematic variables compared to traditional steel shoes. More background information on The hoof, Hoof management and Equine locomotion biomechanics are included in appendix 3. This work will focus on the analysis of kinematic parameters extracted from hoof mounted IMU sensors, on a straight line, on hard surface and at trot, one day after the application of horseshoes.

The following hypothesis was tested:

$H_0$ = There is no significant difference in kinematic hoof parameters between an steel horseshoe and a 3D printed horseshoe on a straight line on hard surface at trot one day after the application of horseshoes.

$H_1$ = There is a significant difference in parameters describing impact vibrations between steel shoe- and 3D printed horseshoe condition on a straight line on hard surface at trot one day after the application of horseshoes.

## II.   Material and methods

This randomised cross-over trial was approved by the local ethics committee in compliance with the Dutch Act on Animal Experimentation (project no. (AKROP/AVD) 10801-2020-07).

**Horses**

Six rider-sound horses owned by Utrecht University (UU), were included in this study. The study group consisted of all mares with a mean body mass of (average ± standard deviation) 581±37 kg, a mean height of 161±4cm and a mean age of 13±2 years. During this project, the horses were used for teaching purposes and regularly at the riding school for veterinary students as usual. The measurements took place at Utrecht University, a familiar environment for the horses.

**Shoeing regime**

The horses were divided into three groups, and each consisting of two individuals. The pairs would follow a different shoeing regime, consisting of three shoeing-cycles in a random chosen order, as described in **Table 1.** Experienced farriers from Utrecht University shod the horses every 7-weeks, with either 3D-printed shoes, or traditional steel shoes, on the front hooves. The same farrier trimmed and shod the same horses during the entire research project to avoid bias.

*Table 1: Overview shoeing-cycles*

| Horse | 1st shoeing-cycle | 2nd shoeing-cycle | 3rd shoeing-cycle |
|---|---|---|---|
| **H1 & H7** | 3D-printed horseshoes | Traditional steel-shoes | Traditional steel-shoes |
| **H3 & H4** | Traditional steel-shoes | 3D-printed horseshoes | Traditional steel-shoes |
| **H5 & H6** | Traditional steel-shoes | Traditional steel-shoes | 3D-printed horseshoes |

The 3D-printed horseshoes used for this project have been developed by the department of clinical science at UU. The 3D-printed horseshoes were made of a plastic composition, thermoplastic elastomer, Hytrel® from DuPon®. The 12 mm thick sole was printed in two colours, changing every 1mm, to ease the monitoring of the wearing of the horseshoe. The weight of the 3D printed horseshoes was 224±24gr. The hooves were scanned with a 3D scanner after trimming and the obtained file was used to design the shoes digitally. Printing two sets of 3D- shoes for the front hooves took three days. The front hooves were therefore bare between the trimming and the application of the shoes. To minimize wearing of the bare hoof, the horses were put on three days of box-rest with hoof bandages. The 3D-printed shoes, as seen in **Figure 1**, have a large sole surface, and a large area that covers the outer hoof wall, which makes it

possible to glue the shoe to the hoof. The 3D-printed shoes were glued onto the hooves with Shufit® glue from Glue-U®.



*Figure 1: Lateral and palmar view of the left front hoof of horse 1, the day of shoeing with 3D-printed horseshoes.*

The traditional steel shoes used for this project from Mustad® had one toe-clip, an 8 mm thick sole and normal size branches, as seen in **Figure 2**. The weight of the shoe was 472±85gr. The 3 days of box-rest, with hoof bandages, between trimming and shoeing were adapted to the steel-shoe cycles, to provide similar conditions as for the 3D printed shoes. The steel shoes were fitted to the hooves by the farrier after a regular trimming and nailed to the hoof with nails form Mustad®.



*Figure 2: Lateral and palmar view of the left front hoof of horse 5, the day of shoeing with steel shoes.*

## Data collection

### *Equipment for motion analysis*

The objective gait analysis system EquiMoves® (EquiMoves®, the Netherlands) was used to collect kinematic data of the horses. The EquiMoves® system works by recording the motion of the horse from synchronized wireless IMUs (Bosch et al. 2018). The IMUs consisted

9

of 3D high-g and 3D low-g accelerometers with measurement ranges of +/-200g and +/-16g respectively, as well as a 3D gyroscope with a range of +/-2000dps.

An overview of the equipment attached to one of the horses participating in the study, is shown in **Figure 3**. The IMU's wirelessly transmitted motion data to the EquiMoves® app, which was running on a laptop nearby. The collected data was saved in the EquiMoves® app, additionally stored in the sensors as backup in case a problem occurred with the software. The straight-line segments at trot were automatically labelled by the EquiMoves® software. For some measurements Inertia Studio's ®, the precursor software of Equimoves ®, was used due to software issues. A sampling frequency of 1000 Hz was set for the sensors on the hooves. A total of 9 sensors was used. However as previously stated, this paper will focus on the data from the hoof-sensors only. The hoof sensors were attached to the dorsal hoof wall by two-sided tape and secured to the hoof by duct-tape. **Figure 4** illustrates the placement of a hoof sensor and the directions of data collection by the sensor.



*Figure 3: An overview of the equipment attached to one of the horses participating.*
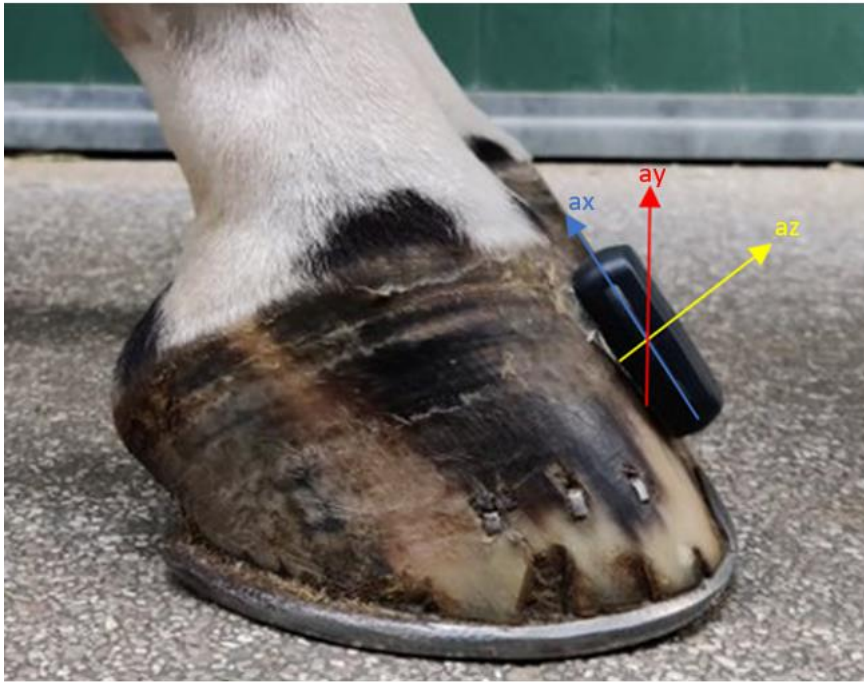
*Figure 4: Attachment of an EquiMoves® sensor to the dorsal hoof wall. Blue arrow shows the proximodistal direction (ax), red arrow shows the mediolateral direction (ay), and yellow arrow shows dorsopalmar direction (az).*

*Measuring protocol*

The horses were measured one by one in random order by an experienced handler after a 5-minute in-hand warm-up. A 10 second stand still period took place before every trial, for software calibration purposes. The measurements were first executed on soft surface, Agterberg composition, followed by repeating the measurements on hard surface, brick. The kinematic measurements were collected at walk and trot, first on a straight line, thereafter on a circle with a 5m radius on both leads. The horses were encouraged to move at their preferred speed. This measurement regime was executed to ensure that at least 25 strides were collected per measurement. This paper will focus on the measurements one day after shoeing, on straight line on hard surface at trot.

**Data processing**

Due to sensor defect, data from left front hoof sensor was lost. This paper therefore focuses on the data obtained from right front hoof sensor only.

Straight line and trot data was automatically labelled by the EquiMoves® app (Bosch et al. 2018). From these segments, the hoof impacts indices were manually selected, based on 3D high-g acceleration and 3D rotation rate signals.

Then, the IMU signals were extracted on a window of 100ms around the impact index, being 50ms before and 50ms after the impact, to be seen in **Figure 5**. For each horse and each condition, 10 impacts were randomly selected and used to extract the impact parameters described in the following sections.

## Data analysis

Five kinematic parameters: Min, Max, Energy, PeakPos and PeakNeg, were extracted from impact curves and analysed in this study. **Figure 5** gives an illustration of impact curves and the extracted parameters: Min, Max, PeakPos and PeakNeg, where the average impact is illustrated with a bold line, while the standard deviation is illustrated with a dotted line. The red and the black circles represent the Max and Min value of the amplitude respectively. The green box gives the area from which PeakNeg counts are extracted, while the blue box gives the area from which PeakPos counts are extracted.
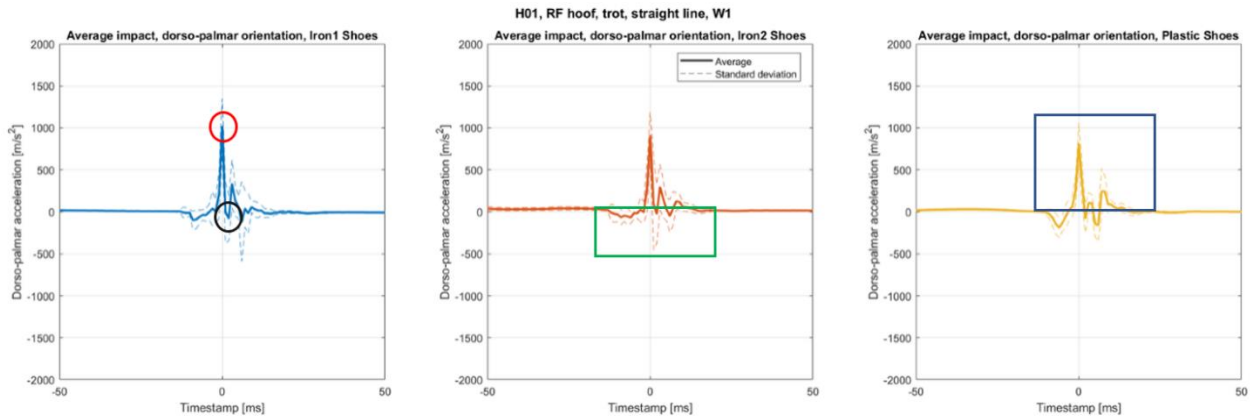


*Figure 5: Examples of impact curves for Steel1, Steel2 and Plastic conditions. The average impact is in bold line, and the standard deviation is in dotted line. The red and the black circles represent the Max and Min value of the amplitude respectively, and the green box gives the area from which PeakNeg counts are extracted, while the blue box gives the area from which PeakPos counts are extracted.*

Further description of these parameters is shown in **Table 2**. All parameters were measured in proximodistal (ax), mediolateral (ay) and dorsopalmar (az) direction.

*Table 2: Description of the parameters measured and analysed.*

| Parameter | Unit | Description |
|---|---|---|
| Min | m/s2 | Minimum value amplitude |
| Max | m/s2 | Maximum value amplitude |
| PeakPos counts | Count | Number of peaks on the positive side of the signal |
| PeakNeg counts | Count | Number of peaks on the negative side of the signal |
| Energy | $(m/s2)^2$ | Energy |

## Statistical analysis

Open software R-studio (version, RStudio (2020), Boston MA, USA) was used for statistical analysis of the data by in-house codes. Impacts that deviated more than two standard deviations from the mean were excluded from further analysis, regarded as outliers.

A linear mixed effect model was used to determine the effect of shoeing-condition on the kinematic parameters extracted with Horse as a random effect and Shoes type and Stride frequency as fixed effects. Data was tested for normality for each variable by plotting the residuals from the linear mixed effect models in QQ plots, density plots, and Gaussian plots. The results obtained with Steel-shoe condition were set as baseline measurement, and the Plastic-shoe condition as intervention. The results of the linear mixed model were considered as significant when P<0.05 and were expressed as effect estimate (estimate) with the correlated standard deviation (SE).

# III.   Results

The results of the linear mixed models are summarised in **Table 3**. Only the significant results will be described in this section. All other results will be included in the appendix.

**Max**

The Max value of the signal was significant larger for Steel2 condition in mediolateral direction (145.25 m/s2, p-value=0.049) and in dorsopalmar direction for Steel1 (263.24m/s2, p-value=0.0001) compared to Plastic condition (see **Figure 6**).

**PeakPos and PeakNeg**

When describing results for PeakPos and PeakNeg parameters, the PeakPos and PeakNeg values were significantly different in dorsopalmar direction only. The PeakPos and PeakNeg counts were less for Steel1 condition (-1.58148, p-value=0.01742 and -1.56364, p-value=0.01888 respectively) compared to Plastic condition (see **Figure 7**).

**Energy**

The signal Energy was significantly larger in mediolateral direction for Steel 2 condition compared to Plastic condition (4673.63 $(m/s2)^2$, p-value=0.0107). In addition, the Energy was significantly larger for Steel 2 condition in dorsopalmar direction (6162.13$(m/s2)^2$, p-value=0.0149) compared to Plastic condition (see

**Figure** *8*).

*Table 3: Results for the linear mixed effect models describing the impact in proximodistal-, dorsopalmar- and mediolateral direction expressed as effect estimate(estimate) with correlated standard error (SE). Significant p-values are marked in red with a star.*

**Proximodistal direction-ax**

| variable | unit | Difference Steel1-Steel2 | | | Difference Steel1-Plastic | | | Difference Steel2-Plastic | | |
|---|---|---|---|---|---|---|---|---|---|---|
| | | estimate | SE | p-value | estimate | SE | p-value | estimate | SE | p-value |
| Min_ax | m/s2 | -25.55 | 43.46 | 0.83 | -32.91 | 36.51 | 0.64 | -7.37 | 41.31 | 0.98 |
| Max_ax | m/s2 | 49.20 | 81.59 | 0.82 | 128.77 | 66.45 | 0.13 | 79.57 | 76.93 | 0.56 |
| PeakPos_ax | Count | 0.21 | 0.49 | 0.90 | 0.83 | 0.39 | 0.09 | 0.61 | 0.46 | 0.38 |
| PeakNeg_ax | Count | -0.13 | 0.46 | 0.96 | 0.79 | 0.37 | 0.08 | 0.92 | 0.43 | 0.09 |
| Energy_ax | $(m/s2)^2$ | 1828.16 | 2717.45 | 0.78 | 3495.22 | 2213.33 | 0.26 | 1667.07 | 2562.14 | 0.79 |

**Mediolateral direction-ay**

| variable | unit | Difference Steel1-Steel2 | | | Difference Steel1-Plastic | | | Difference Steel2-Plastic | | |
|---|---|---|---|---|---|---|---|---|---|---|
| | | estimate | SE | p-value | estimate | SE | p-value | estimate | SE | p-value |
| Min_ay | m/s2 | 66.04 | 67.27 | 0.59 | -43.48 | 54.02 | 0.70 | -109.52 | 63.19 | 0.20 |
| Max_ay | m/s2 | -46.73 | 65.29 | 0.75 | 98.52 | 52.36 | 0.15 | 145.25 | 61.31 | 0.04973* |
| PeakPos_ay | Count | 0.73 | 0.85 | 0.67 | 0.80 | 0.68 | 0.47 | 0.08 | 0.80 | 0.80 |
| PeakNeg_ay | Count | 0.72 | 0.87 | 0.68 | 0.98 | 0.69 | 0.34 | 0.25 | 0.81 | 0.81 |
| Energy_ay | $(m/s2)^2$ | -2070.53 | 1695.50 | 0.44 | 2603.10 | 1357.80 | 0.14 | 4673.64 | 1591.60 | 0.01066* |

**Dorsopalmar direction-az**

| variable | unit | Difference Steel1-Steel2 | | | Difference Steel1-Plastic | | | Difference Steel2-Plastic | | |
|---|---|---|---|---|---|---|---|---|---|---|
| | | estimate | SE | p-value | estimate | SE | p-value | estimate | SE | p-value |
| Min_az | m/s2 | -6.72 | 54.96 | 0.99 | -92.02 | 45.60 | 0.11 | -85.30 | 52.07 | 0.23 |
| Max_az | m/s2 | 106.07 | 76.27 | 0.35 | 263.24 | 61.67 | 0.0001* | 157.17 | 71.77 | 0.08 |
| PeakPos_az | Count | -0.78 | 0.71 | 0.52 | -1.58 | 0.57 | 0.01742* | -0.81 | 0.67 | 0.45 |
| PeakNeg_az | Count | -0.78 | 0.71 | 0.51 | -1.56 | 0.57 | 0.01888* | -0.78 | 0.67 | 0.48 |
| Energy_az | $(m/s2)^2$ | 2920.80 | 2690.69 | 0.52 | 6162.13 | 2184.13 | 0.01491* | 3241.33 | 2534.69 | 0.41 |
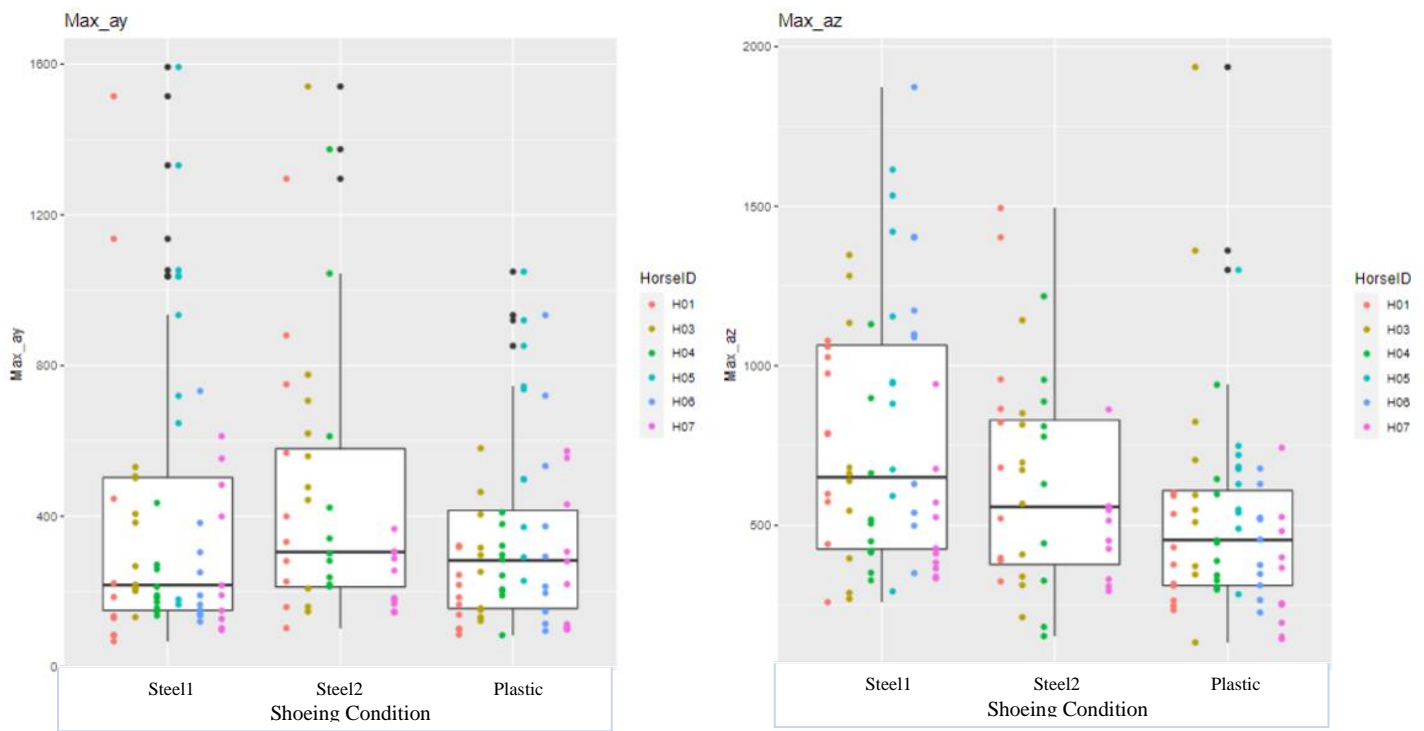
*Figure 6: Figures illustrating how the mean of the amplitude Max values change for each horse between the Steel conditions and Plastic condition, mediolateral-ay and dorsopalmar-az direction.*
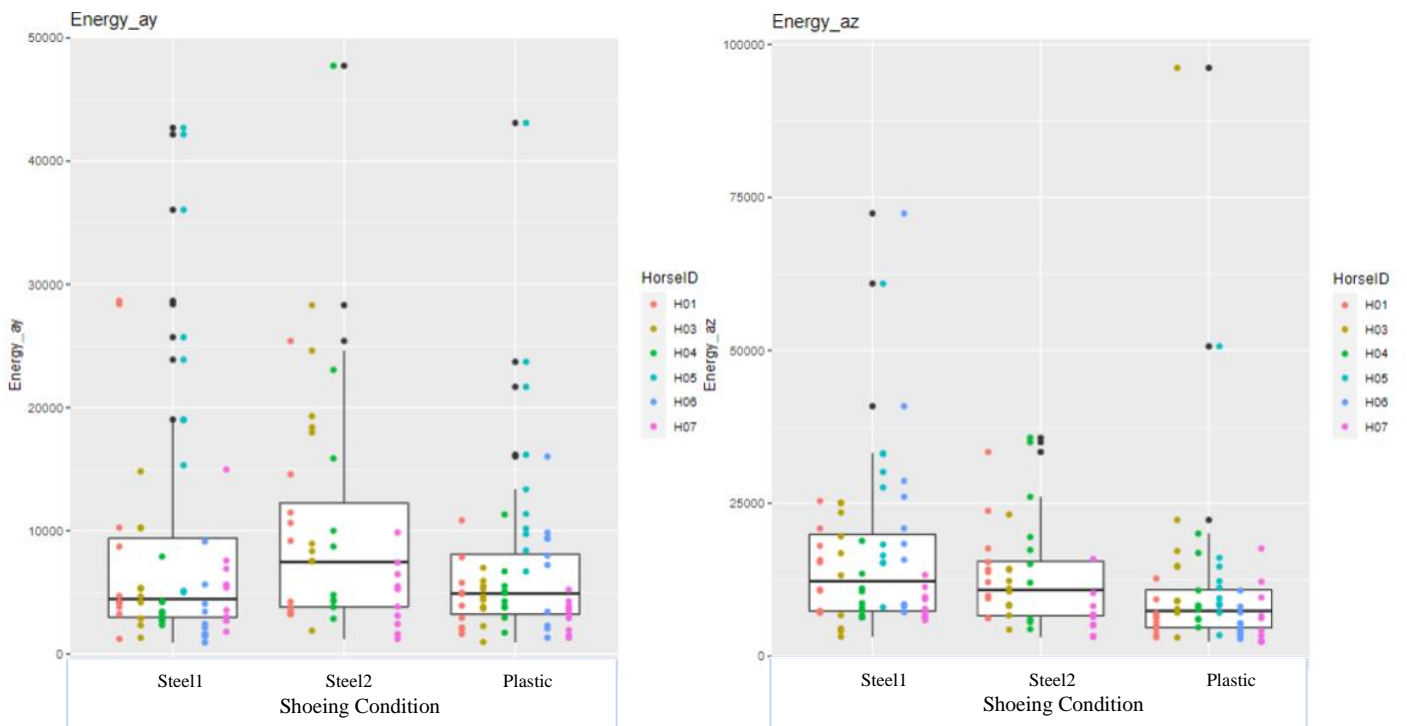


*Figure 7: Figures illustrating how the mean of the signal Energy change for each horse between the Steel conditions and Plastic condition, mediolateral-ay and dorsopalmar-az direction.*

15
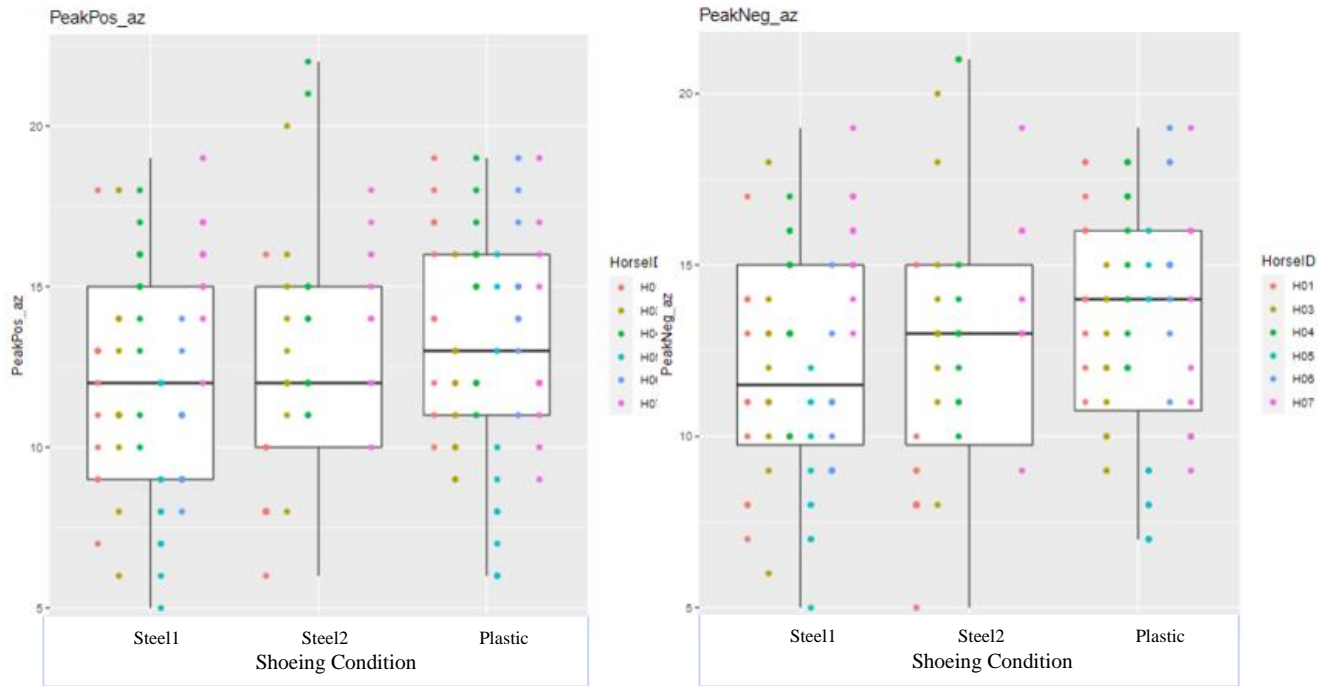
*Figure 8: Figures illustrating how the mean of the values PeakPos and PeakNeg change for each horse between the Steel conditions and Plastic condition, dorsopalmar-az direction.*

# IV. Discussion

The objective of the present study was to investigate the influence of the newly developed 3D-printed horseshoes on hoof kinematic parameters.

It was hypothesised that the hoof-kinematic impact vibration parameters for 3D-printed condition would significantly differ from the Steel conditions on straight line and on hard surface at trot. The larger Max acceleration values for Steel1 and Steel2 condition, in dorsopalmar and mediolateral direction respectively, could indicate that the impact vibrations were smaller for Plastic condition compared to Steel conditions. In both dorsopalmar and mediolateral direction, the signal Energy was smaller for Plastic condition compared to Steel2 condition. The higher amount of PeakPos and PeakNeg counts for Plastic condition in dorsopalmar direction compared to Steel1 condition simultaneously with the lesser Max acceleration values and lesser signal energy, suggests that the impact was more distributed in dorsopalmar direction with the 3D-printed horseshoes. The combination of the findings on the mentioned kinematic hoof parameters imply that the 3D-printed horseshoes had a more smoothly impact compared to the traditional steel shoes.

These results are comparable to those provided in the study of Back et al., 2006 and the study of Moore et al., 2019. In the study of Back et al., 2006 it was concluded that polyurethane shoes modify impact at hoof level compared to traditional steel shoes and unshod condition on asphalt. A triaxial piezoelectric accelerometer was fixed to the lateral hoof wall to measure accelerations at a sampling rate of 10kHz. The maximum amplitude of horizontal and vertical, forward/backward accelerations was lowest with polyurethane shoes($p<0.05$). In the study of Moore et al., 2019, steel horseshoes with a polyurethane layer were compared to a traditional steel shoe at asphalt. In this study they used triaxial accelerometers, mounted onto the dorsal hoof wall, from two different systems with sampling rates at 50 Hz and 148Hz. The results showed that the polyurethane shoes had significant reduced decelerations at stance phase ($p=0.06$).

Some of the results acquired in this study were significantly different between Steel1 condition compared to Plastic condition, while not significantly different between Steel2 condition compared to Plastic condition, and vice versa, even though the estimates were of comparable amplitudes (**Table 3**). This differences between Steel1 and Steel2 conditions complicated the analysis and interpretation of the results. One possible explanation could be that the inter- and intra-horse variation had more influence on the hoof impact parameters than the effect from the different kind of horseshoes compared in this study. This could be related to the non-homogenous study population, consisting of six horses of different breeds. Compared to other studies, the study of Back et al., 2006 used 12 Dutch warmblood horses, while Moore et al., 2019 on the other hand only used four horses, two trotters, and two warmbloods. Another explanation could be that the measurement method used in this project was insufficient for the parameters analysed. For example: the sampling frequency in this study was set at 1000Hz. Other researchers have used a sampling frequency of 10kHz as for Back et al., 2006, while the research of Moore et al., 2019 used sampling frequencies of 50 Hz and 148 Hz. An increased sampling frequency and preferably a larger, more homogenous study population might have been beneficial to detect and/or explain the differences between the shoeing conditions.

**Main limitations**

One of the main limitations of this study was the size and composition of the study population, which should have been larger and more homogenous. A larger study population would be less sensitive for unforeseen dropouts and missing measurements. The variation in breed might have contributed to a larger inter-horse variation, and thereby making the comparison between horses less accurate. Furthermore, the horses in this study were deemed rider-sound at the beginning of the project. Research of Müller-Quirin et al., 2020 concluded that rider/owner sound horses often deviate from subjective and objective lameness assessments (Müller-Quirin et al., 2020). Preferably, the horses should have gone through a locomotion evaluation by a veterinarian prior to the project.

There were some limitations regarding study design: sensor attachment, handler effect, and the organisation of the application of the 3D-printed horseshoes. First, the sensors could have been attached in closer contact with the hoof, to ensure less artefacts. Ideally, the sensors should have been mounted straight onto the hoof, and not remain in the black plastic cases the sensors came with. The plastic case made it difficult to closely attach the sensor to the dorsal hoof wall. Moreover, differences between the hoof conformation of the horses and the shoeing, e.g., shape and glue from the 3D-shoes, led to less space left to attach the sensor properly. Secondly, it would have been beneficial to use the same handler every time, as a different handler might influence the horses' moving pattern. In this study, it was not possible to use the same handler every time due to logistical reasons. Lastly, the organisation and application of the 3D-printed horseshoes is still not fully objective or automated as a farrier is still needed for the trimming of the hooves. Due to the time necessary to print the shoes, the horses were put on box-rest for three days with hoof bandages. Staying in hoof bandages at box rest might not be desired in all cases as it limits the possibility of training and movement. Making it possible to print the 3Dprinted shoes faster would be beneficial for the possibility of adapting the use of these shoes outside an experimental setting.

The 3D-printed horseshoe itself did not only differ in material from the traditional Steel shoe. It must be mentioned that the weight and the conformation of the horseshoe was different between the steel shoe (472±85gr) and plastic shoe (224±24gr). In the study of Balch et al., 1996 the mass of the horseshoe was doubled from 348gr to 869gr to investigate the effect on kinematic parameters. The weight influenced the maximal height of the hoof and caused a more "animated trot" (Balch et al., 1996). However, the effects of weight and weight differences of horseshoes on hoof impact vibration parameters is unknown. The study of Stutz et al. 2018 compared steel horseshoes with different conformation to one another and to a barefoot condition. The outcome of this study showed significant differences between shod and unshod horses, but no significant difference between the shod conditions (Stutz et al. 2018). It would have been interesting to compare the 3D-printed horseshoes to a barefoot condition as the conclusion from Stutz et al., 2018 were that the presence of a horseshoe influenced kinematics more than the geometrical differences between the different horseshoes examined.

Regarding data analysis, the hoof impacts indices were manually selected from the segments provided from EquiMoves ® and Inertia Studios ®, which leaves room for human error. Preferably, the selection of hoof impact indices should have been automated. This research has focused on comparing discrete variables extracted from the impact curves (see **Figure 5**). It would have been interesting to compare continuous whole curves, as extracted

variables only represent a small part of a horse's locomotion pattern. The study of Smit et al., 2021 compared continuous data analysis to analysis of discrete values. The research concluded that the use of continuous data provides additional information, regarding gait adaptation to bilateral lameness (Smit et al., 2021).

**Future research**

The described differences in the present study suggest that the use of 3D-printed horseshoes modify impact by decreasing impact vibrations and are furthermore of no harm to equines. These findings open for further research into the possibilities of 3D-printed horseshoes. Future research projects should take the limitations of this study into consideration, for example a more detailed horse-selection procedure including a locomotion evaluation. This is especially important if wanting to study the effect of 3D-printed horseshoes on hoof related pathologies.

# V.   Conclusion

This present study is the initial phase of research on 3D-printed horseshoes. The presented results on hoof kinematic parameters suggest that these 3D-printed shoes modify impact by reducing the impact vibrations at trot on straight line and hard surface. Future research is encouraged to reveal more about the possibilities of the use of 3D-printed horseshoes.

# References

Arkell, M., R. M. Archer, F. J. Guitian, and S. A. May. 2006. 'Evidence of Bias Affecting the Interpretation of the Results of Local Anaesthetic Nerve Blocks When Assessing Lameness in Horses'. *The Veterinary Record* 159 (11): 346–49. https://doi.org/10.1136/vr.159.11.346.

Back, Willem, and Hilary M Clayton. 2013. *Equine Locomotion*. Edinburgh [Scotland]; New York: Saunders Elsevier.(pp 147-174)

Back, W., van Schie, M. H. M., & Pol, J. N. (2006). Synthetic shoes attenuate hoof impact in the trotting warmblood horse. *Equine and Comparative Exercise Physiology*, *3*(3), 143–151. https://doi.org/10.1017/ecp200691

Balch, O. K., D. Butler, and M. A. Collier. 1997. 'Balancing the Normal Foot: Hoof Preparation, Shoe Fit and Shoe Modification in the Performance Horse'. *Equine Veterinary Education* 9 (3): 143–54. https://doi.org/10.1111/j.2042-3292.1997.tb01295.x.

Bolink, S. A. A. N., H. Naisas, R. Senden, H. Essers, I. C. Heyligers, K. Meijer, and B. Grimm. 2016. 'Validity of an Inertial Measurement Unit to Assess Pelvic Orientation Angles during Gait, Sit–Stand Transfers and Step-up Transfers: Comparison with an Optoelectronic Motion Capture System*'. *Medical Engineering & Physics* 38 (3): 225–31. https://doi.org/10.1016/j.medengphy.2015.11.009.

Bosch, Stephan, Filipe Serra Bragança, Mihai Marin-Perianu, Raluca Marin-Perianu, Berend Jan Van der Zwaag, John Voskamp, Willem Back, René Van Weeren, and Paul Havinga. 2018. 'EquiMoves: A Wireless Networked Inertial Measurement System for Objective Examination of Horse Gait'. *Sensors* 18 (3): 850. https://doi.org/10.3390/s18030850.

Clayton, Hilary M., and Sarah-Jane Hobbs. 2017. 'The Role of Biomechanical Analysis of Horse and Rider in Equitation Science'. *Applied Animal Behaviour Science*, Special Issue on Equitation Science in Practice, 190 (May): 123–32. https://doi.org/10.1016/j.applanim.2017.02.011.

Colles, C. M. 1989. 'The Relationship of Frog Pressure to Heel Expansion'. *Equine Veterinary Journal* 21 (1): 13–16. https://doi.org/10.1111/j.2042-3306.1989.tb02082.x.

Davies, H. M. S. 2002. 'No Hoof, No Horse! The Clinical Implications of Modelling the Hoof Capsule'. *Equine Veterinary Journal* 34 (7): 646–47. https://doi.org/10.2746/042516402776250432.

Douglas, J. E., T. L. Biddick, J. J. Thomason, and J. C. Jofriet. 1998. 'Stress/Strain Behaviour of the Equine Laminar Junction.' *Journal of Experimental Biology* 201 (15): 2287–97.

'Dyce, Sack, and Wensing's Textbook of Veterinary Anatomy | 2018

Dyhre-Poulsen, P., H. H. Smedegaard, J. Roed, and E. Korsgaard. 1994. 'Equine Hoof Function Investigated by Pressure Transducers inside the Hoof and Accelerometers Mounted on the First Phalanx'. *Equine Veterinary Journal* 26 (5): 362–66. https://doi.org/10.1111/j.2042-3306.1994.tb04404.x.

Eichelberger, Patric, Matteo Ferraro, Ursina Minder, Trevor Denton, Angela Blasimann, Fabian Krause, and Heiner Baur. 2016. 'Analysis of Accuracy in Optical Motion Capture – A Protocol for Laboratory Setup Evaluation'. *Journal of Biomechanics* 49 (10): 2085–88. https://doi.org/10.1016/j.jbiomech.2016.05.007.

Eliashar, Ehud. 2007. 'An Evidence-Based Assessment of the Biomechanical Effects of the Common Shoeing and Farriery Techniques'. *Veterinary Clinics of North America: Equine Practice*, Evidence-based Veterinary Medicine, 23 (2): 425–42. https://doi.org/10.1016/j.cveq.2007.03.010.

Guerra-filho, Gutemberg B. 2005. 'Optical Motion Capture: Theory and Implementation'. *Journal of Theoretical and Applied Informatics (RITA* 12: 61–89.

Gustås, P., C. Johnston, L. Roepstorff, and S. Drevemo. 2001. 'In Vivo Transmission of Impact Shock Waves in the Distal Forelimb of the Horse'. *Equine Veterinary Journal* 33 (S33): 11–15. https://doi.org/10.1111/j.2042-3306.2001.tb05350.x.

Hammarberg, M., A. Egenvall, T. Pfau, and M. Rhodin. 2016. 'Rater Agreement of Visual Lameness Assessment in Horses during Lungeing'. *Equine Veterinary Journal* 48 (1): 78–82. https://doi.org/10.1111/evj.12385.

Heel, M. C. V. Van, A. Barneveld, P. R. Van Weeren, and W. Back. 2004. 'Dynamic Pressure Measurements for the Detailed Study of Hoof Balance: The Effect of Trimming'. *Equine Veterinary Journal* 36 (8): 778–82. https://doi.org/10.2746/0425164044847993.

Heel, M. C. V. van, M. Moleman, A. Barneveld, P. R. van Weeren, and W. Back. 2005. 'Changes in Location of Centre of Pressure and Hoof-Unrollment Pattern in Relation to an 8-Week Shoeing Interval in the Horse'. *Equine Veterinary Journal* 37 (6): 536–40. https://doi.org/10.2746/042516405775314925.

Hinterhofer, C., N. Weißbacher, H.H.F. Buchner, Christian Peham, and C. Stanek. 2006. 'Motion Analysis of Hoof Wall, Sole and Frog under Cyclic Load in Vitro: Deformation of the Equine Hoof Shod with Regular Horse Shoe, Straight Bar Shoe and Bare Hoof'. *Pferdeheilkunde* 22 (May): 314–19. https://doi.org/10.21836/PEM20060311.

Hood, D. M., D. Taylor, and I. P. Wagner. 2001. 'Effects of Ground Surface Deformability, Trimming, and Shoeing on Quasistatic Hoof Loading Patterns in Horses'. *American Journal of Veterinary Research* 62 (6): 895–900. https://doi.org/10.2460/ajvr.2001.62.895.

Kai, Makoto, Osamu Aoki, Atsushi Hiraga, Hironori Oki, and Mikihiko Tokuriki. 2000. 'Use of an Instrument Sandwiched between the Hoof and Shoe to Measure Vertical Ground Reaction Forces and Three-Dimensional Acceleration at the Walk, Trot, and Canter in Horses'. *American Journal of Veterinary Research* 61 (8): 979–85. https://doi.org/10.2460/ajvr.2000.61.979.

Keegan, K. G., E. V. Dent, D. A. Wilson, J. Janicek, J. Kramer, A. Lacarrubba, D. M. Walsh, et al. 2010. 'Repeatability of Subjective Evaluation of Lameness in Horses'. *Equine Veterinary Journal* 42 (2): 92–97. https://doi.org/10.2746/042516409X479568.

Keegan, Kevin G. 2007. 'Evidence-Based Lameness Detection and Quantification'. *Veterinary Clinics of North America: Equine Practice*, Evidence-based Veterinary Medicine, 23 (2): 403–23. https://doi.org/10.1016/j.cveq.2007.04.008.

Kuiper, R. van Nieuwstadt 2016. ' Het klinisch onderzoek van paard en landbouwhuisdieren'.

Leśniak, Kirsty, Jane Williams, Kerry Kuznik, and Peter Douglas. 2017. 'Does a 4–6 Week Shoeing Interval Promote Optimal Foot Balance in the Working Equine?' *Animals : An Open Access Journal from MDPI* 7 (4). https://doi.org/10.3390/ani7040029.

Merkens, H. W., H. C. Schamhardt, Geertruda J. V. M. Van Osch, and A. J. Van Den Bogert. 1993. 'Ground Reaction Force Patterns of Dutch Warmblood Horses at Normal Trot'. *Equine Veterinary Journal* 25 (2): 134–37. https://doi.org/10.1111/j.2042-3306.1993.tb02923.x.

Moleman, M., M. C. V. Van Heel, P. R. Van Weeren, and W. Back. 2006. 'Hoof Growth between Two Shoeing Sessions Leads to a Substantial Increase of the Moment about the Distal, but Not the Proximal, Interphalangeal Joint'. *Equine Veterinary Journal* 38 (2): 170–74. https://doi.org/10.2746/042516406776563242.

Moore, Lauren Veneta, Rebeka Roza Zsoldos, and Theresia Franziska Licka. 2019. 'Trot Accelerations of Equine Front and Hind Hooves Shod with Polyurethane Composite Shoes and Steel Shoes on Asphalt'. *Animals : An Open Access Journal from MDPI* 9 (12). https://doi.org/10.3390/ani9121119.

Moorman, Valerie J., Raoul F. Reiser II, C. Wayne McIlwraith, and Chris E. Kawcak. 2012. 'Validation of an Equine Inertial Measurement Unit System in Clinically Normal Horses during Walking and Trotting'. *American Journal of Veterinary Research* 73 (8): 1160–70. https://doi.org/10.2460/ajvr.73.8.1160.

O'Grady, Stephen E. 2017. 'Therapeutic Shoes: Application of Principles'. In *Equine Laminitis*, 341–53. John Wiley & Sons, Ltd. https://doi.org/10.1002/9781119169239.ch38.

O'Grady, Stephen E, and Derek A Poupard. 2003a. 'Proper Physiologic Horseshoeing'. *Veterinary Clinics of North America: Equine Practice*, Podiatry, 19 (2): 333–51. https://doi.org/10.1016/S0749-0739(03)00020-8.

———. 2003b. 'Proper Physiologic Horseshoeing'. *Veterinary Clinics of North America: Equine Practice*, Podiatry, 19 (2): 333–51. https://doi.org/10.1016/S0749-0739(03)00020-8.

Oosterlinck, M., M. Dumoulin, E. Van de Water, and F. Pille. 2017. 'Biomechanische aspecten met betrekking tot hoefbeslag bij paarden'. *Vlaams Diergeneeskundig Tijdschrift* 86 (4): 256–65. https://doi.org/10.21825/vdt.v86i4.16187.

Parkes, R. S. V., R. Weller, A. M. Groth, S. May, and T. Pfau. 2009. 'Evidence of the Development of "Domain-Restricted" Expertise in the Recognition of Asymmetric Motion Characteristics of Hindlimb Lameness in the Horse'. *Equine Veterinary Journal* 41 (2): 112–17. https://doi.org/10.2746/042516408X343000.

Pfau, Thilo, Thomas H. Witte, and Alan M. Wilson. 2005. 'A Method for Deriving Displacement Data during Cyclical Movement Using an Inertial Sensor'. *Journal of Experimental Biology* 208 (13): 2503–14. https://doi.org/10.1242/jeb.01658.

Pollitt, C. C. 1992. 'Clinical Anatomy and Physiology of the Normal Equine Foot'. *Equine Veterinary Education* 4 (5): 219–24. https://doi.org/10.1111/j.2042-3292.1992.tb01623.x.

'Riding Soundness-Comparison of Subjective With Objective Lameness Assessments of Owner-Sound Horses at Trot on a Treadmill | Elsevier Enhanced Reader'. n.d. Accessed 9 January 2022. https://doi.org/10.1016/j.jevs.2020.103314.

Rivero, J.-L. L. 2007. 'A Scientific Background for Skeletal Muscle Conditioning in Equine Practice'. *Journal of Veterinary Medicine Series A* 54 (6): 321–32. https://doi.org/10.1111/j.1439-0442.2007.00947.x.

Roepstorff, L., C. Johnston, and S. Drevemo. 1999. 'The Effect of Shoeing on Kinetics and Kinematics during the Stance Phase'. *Equine Veterinary Journal* 31 (S30): 279–85. https://doi.org/10.1111/j.2042-3306.1999.tb05235.x.

———. 2001a. 'In Vivo and in Vitro Heel Expansion in Relation to Shoeing and Frog Pressure'. *Equine Veterinary Journal* 33 (S33): 54–57. https://doi.org/10.1111/j.2042-3306.2001.tb05359.x.

———. 2001b. 'In Vivo and in Vitro Heel Expansion in Relation to Shoeing and Frog Pressure'. *Equine Veterinary Journal* 33 (S33): 54–57. https://doi.org/10.1111/j.2042-3306.2001.tb05359.x.

Serra Bragança, F. M., M. Rhodin, and P. R. van Weeren. 2018. 'On the Brink of Daily Clinical Application of Objective Gait Analysis: What Evidence Do We Have so Far from Studies Using an Induced Lameness Model?' *The Veterinary Journal* 234 (April): 11–23. https://doi.org/10.1016/j.tvjl.2018.01.006.

Smit, Ineke H., Elin Hernlund, Harold Brommer, Paul René van Weeren, Marie Rhodin, and Filipe M. Serra Bragança. n.d. 'Continuous versus Discrete Data Analysis for Gait Evaluation of Horses with Induced Bilateral Hindlimb Lameness'. *Equine Veterinary Journal* n/a (n/a). Accessed 21 November 2021. https://doi.org/10.1111/evj.13451.

Stutz, Joëlle Christina, Beatriz Vidondo, Alessandra Ramseyer, Ugo Ettore Maninchedda, and Antonio M Cruz. 2018. 'Effect of Three Types of Horseshoes and Unshod Feet on Selected Non-Podal Forelimb Kinematic Variables Measured by an Extremity Mounted Inertial Measurement Unit Sensor System in Sound Horses at the Trot under Conditions of Treadmill and Soft Geotextile Surface Exercise'. *Veterinary Record Open* 5 (1). https://doi.org/10.1136/vetreco-2017-000237.

Thomason, Jeffrey J., and Michael L. Peterson. 2008. 'Biomechanical and Mechanical Investigations of the Hoof-Track Interface in Racing Horses'. *Veterinary Clinics of North America: Equine Practice*, Performance Horse Lameness and Orthopedics, 24 (1): 53–77. https://doi.org/10.1016/j.cveq.2007.11.007.

Weishaupt, Michael A., Hermann P. Hogg, Thomas Wiestner, Jachen Denoth, Edgar Stüssi, and Jörg A. Auer. 2002. 'Instrumented Treadmill for Measuring Vertical Ground Reaction Forces in Horses'. *American Journal of Veterinary Research* 63 (4): 520–27. https://doi.org/10.2460/ajvr.2002.63.520.

Weller, R., A. Barstow, H. Price, and T. Pfau. 2018. 'Evidence-Based Farriery – Does It Exist?' *Equine Veterinary Journal* 50 (5): 552–53. https://doi.org/10.1111/evj.12978.

Wilson, A., R. Agass, S. Vaux, E. Sherlock, P. Day, T. Pfau, and R. Weller. 2016. 'Foot Placement of the Equine Forelimb: Relationship between Foot Conformation, Foot Placement and Movement Asymmetry'. *Equine Veterinary Journal* 48 (1): 90–96. https://doi.org/10.1111/evj.12378.

Windolf, Markus, Nils Götzen, and Michael Morlock. 2008. 'Systematic Accuracy and Precision Analysis of Video Motion Capturing Systems--Exemplified on the Vicon-460 System'. *Journal of Biomechanics* 41 (12): 2776–80. https://doi.org/10.1016/j.jbiomech.2008.06.024.

Witte, T. H., K. Knill, and A. M. Wilson. 2004. 'Determination of Peak Vertical Ground Reaction Force from Duty Factor in the Horse (Equus Caballus)'. *Journal of Experimental Biology* 207 (21): 3639–48. https://doi.org/10.1242/jeb.01182.

Yoshihara, E., T. Takahashi, N. Otsuka, T. Isayama, T. Tomiyama, A. Hiraga, and S. Wada. 2010. 'Heel Movement in Horses: Comparison between Glued and Nailed Horse Shoes at Different Speeds'. *Equine Veterinary Journal* 42 (s38): 431–35. https://doi.org/10.1111/j.2042-3306.2010.00243.x.

# Appendices

## Appendix 1: Overview of horses participating
An overview of the horses used in this study and which shoeing regime they followed.

| Horse | Breed | Weight (kg) | Height withers (cm) | Year of birth | Shoeing cycle order |
|---|---|---|---|---|---|
| **H1** | KWPN Tuigpaard | 532 | 161 | 2006 | Plastic- Steel 1 - Steel 2 |
| **H7** | Friesian Horse | 616 | 160 | 2006 | |
| **H3** | KWPN Rijpaard | 608 | 165 | 2009 | Steel 1- Plastic - Steel 2 |
| **H4** | KWPN Rijpaard | 626 | 164 | 2008 | |
| **H5** | KWPN Tuigpaard | 554 | 159 | 2011 | Steel 1- Steel 2 - Plastic |
| **H6** | Irish Piebald & SkewbalI | 547 | 154 | 2007 | |

# Appendix 2: Boxplots

Boxplots of Min, Max, Energy, PeakPos and PeakNeg values not previously included.

PeakPos_ax



PeakPos_ay



PeakNeg_ax



PeakNeg_ay
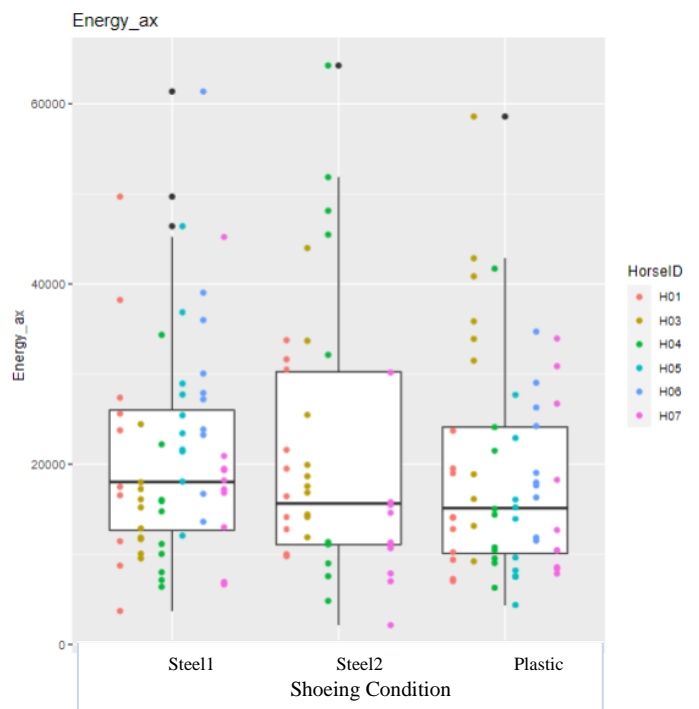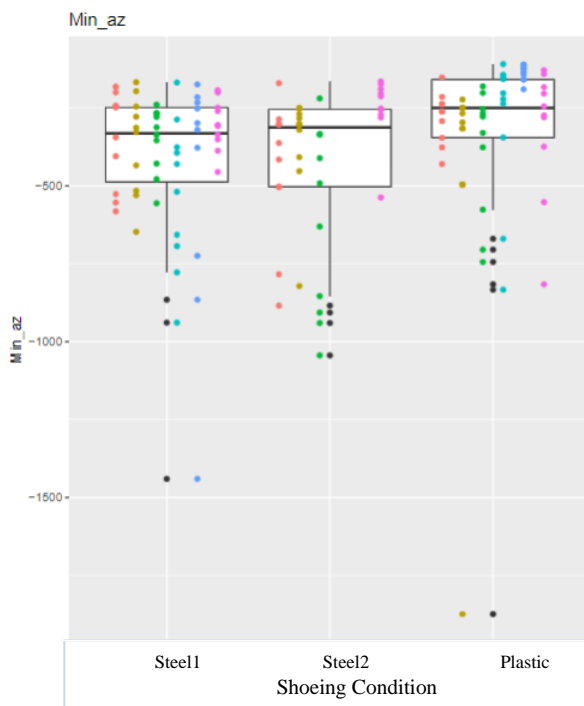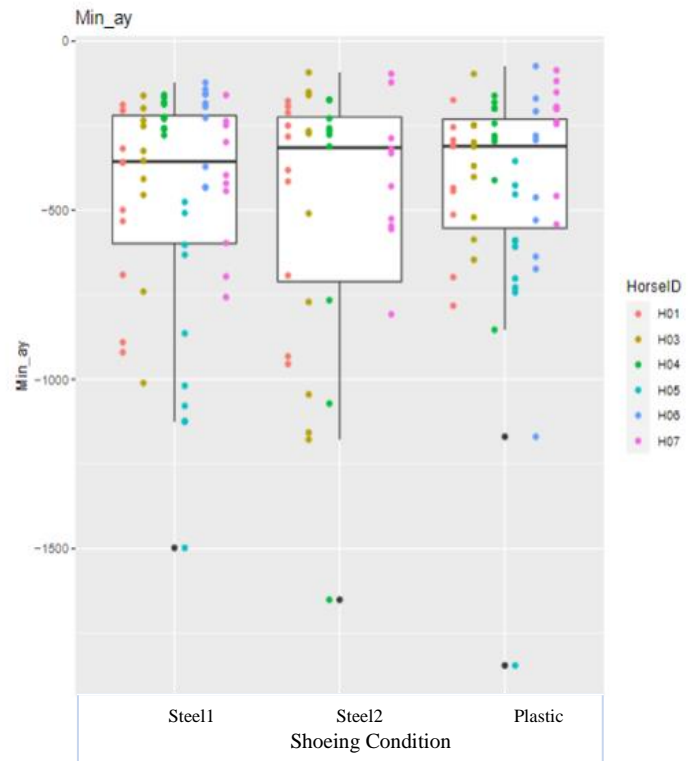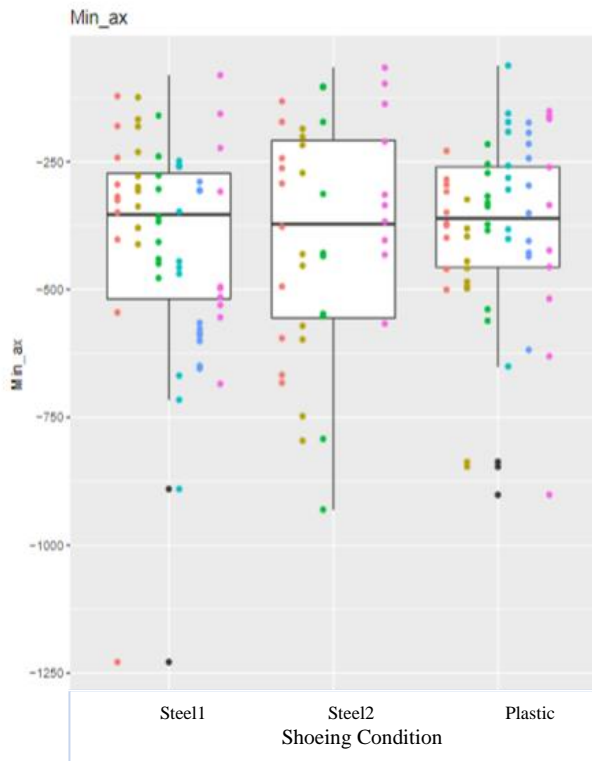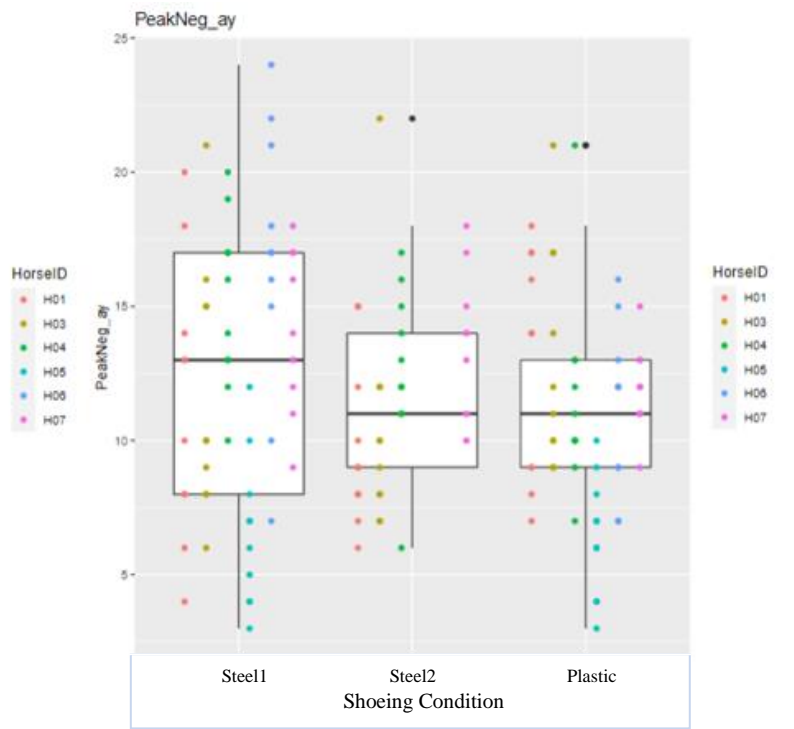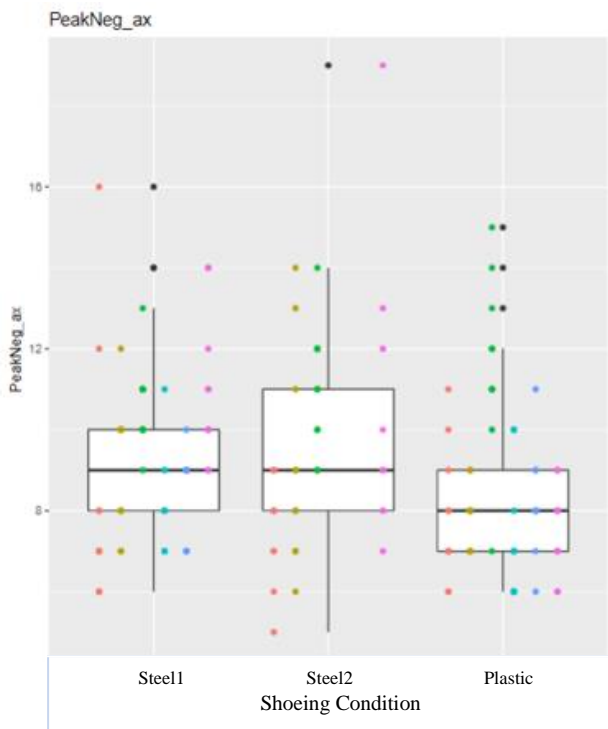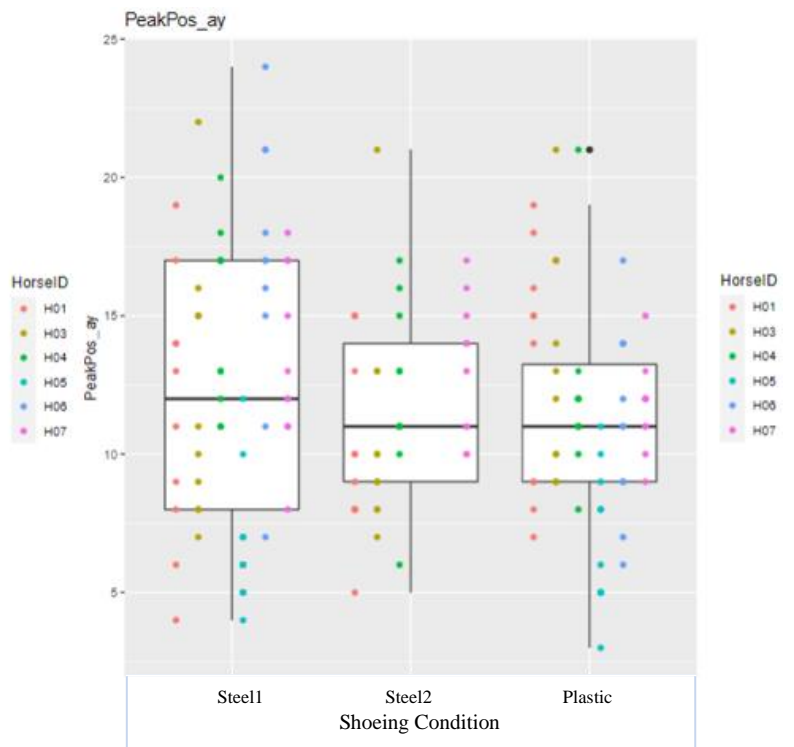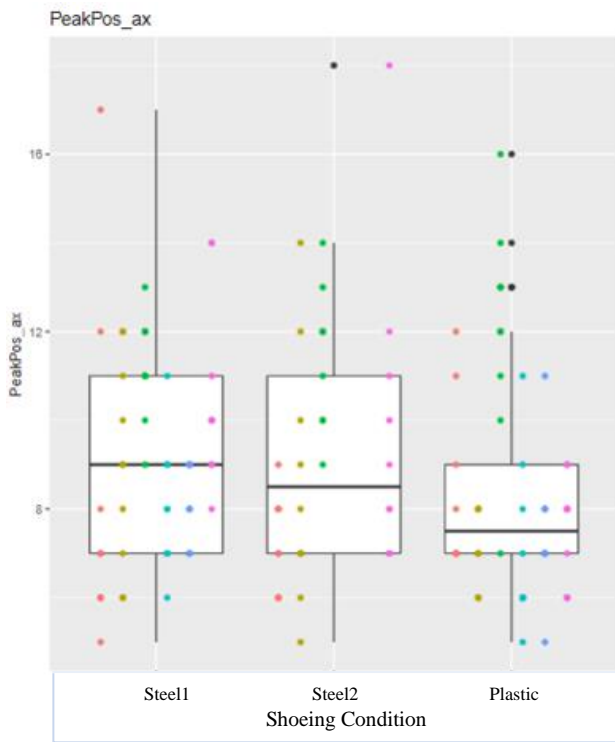
# Appendix 3: Background information

In this section, background information about the hoof, hoof management and equine gait analysis will be given.

## 3.1 The hoof

The hoof is one of the main structures involved in equine locomotion, as it is in direct contact with the surface during every stride. Repeated, abnormal direction of action and/or expose to high magnitude forces, can overload the limb and cause pathologies influencing the equine locomotion (Rivero 2007).

### 3.1.1 Hoof anatomy

The distal extremity of the horse's limb is covered by a hoof capsule (Dyce et al., 2018). The hoof capsule can be divided into the hoof wall, the sole and the frog as seen in **Figure 9**Figure 9. The coronary segment is the junction between skin and hoof, where the hoof wall is created. "The hoof wall grows approximately 1cm every 6 weeks, with the wall at the toe growing faster than at the heels" (Hertsch et al., 1996). The hoof wall is the part of the hoof, which is visible in the standing horse. It forms the dorsal, medial, and lateral aspect of the hoof and can further be divided into toe, heel, and quarters. The wall is at its thickest at the toe, and gradually thins around the quarters towards the heel (Dyce et al., 2018). The junction between the wall and the sole is known as the white line. The sole fills the space between the frog and the hoof wall. It is slightly concave which leaves only the frog, and the distal edge of the hoof wall to be in contact with the ground standing on a hard surface. The frog projects into the sole from behind, closing the gap between the heels (Dyce et al., 2018).
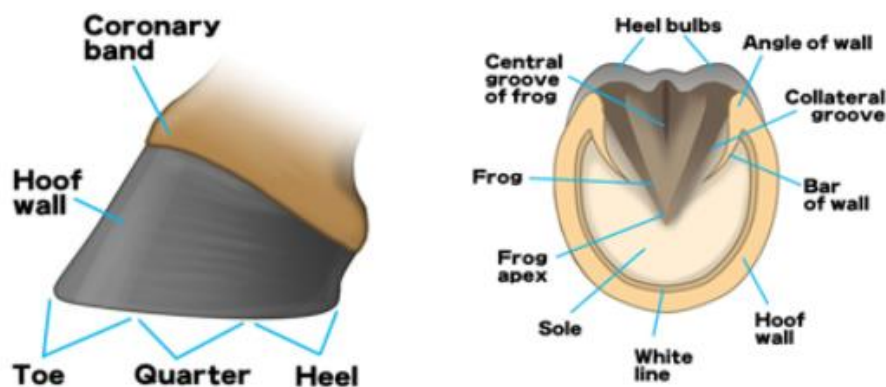


*Figure 9: The superficial structures of the hoof. Adapted from https://www.minnano-jouba.com/mame_chishiki07_en.html 21.11.2021.*

The hoof capsule protects the more sensitive structures within the hoof, as shown in **Figure 10**. The bony segments of the hoof consist of the distal phalanx (P3), a part of the middle phalanx (P2) and the navicular bone (Dyce et al., 2018). The hoof capsule is attached to the distal phalanx (P3) by the interdigitation of the epidermal laminae of the hoof wall with the dermal laminae of the distal phalanx. The deep digital flexor tendon (DDFT) curves around the palmar aspect of the navicular bone before attaching to the distal phalanx. The lateral and medial hoof cartilages are located on either side of the distal phalanx. Between these cartilages lie the digital cushion and a venous plexus (Hoffman et al., 2001; Pietra et al., 2004).
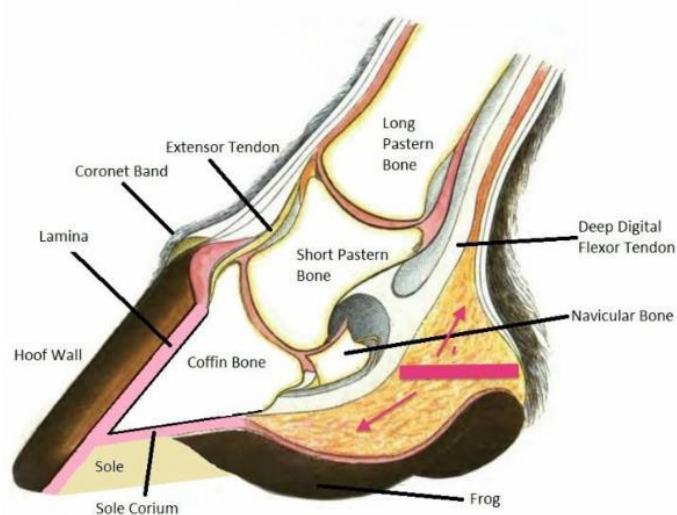
*Figure 10: The deeper structures of the hoof. Adapted from https://www.irongateequine.com/education/laminitis 21.11.2021*

### 3.1.2 Stride biomechanics

A stride can be defined as the time between the hoof touches the ground until the next time, the same hoof, touches the ground. A full stride consists of a stance phase, where the limb is in contact with the surface, and a swing phase, where the limb is not in contact with the surface. The stance phase can be divided into different phases with different biomechanical characteristics; impact-, support- and breakover phase. The swing phase can be divided into: post breakover, mid-swing and pre-impact phase (Back and Clayton 2013; Thomason and Peterson 2008). The following section will further describe the different stride phases.

The pre-impact is the moment just before the hoof hits the ground. The impact phase represents the initial contact of the hoof with the ground, either toe, flatfooted or heel first. It is not possible to see which part of the hoof initially meets the ground with the naked eye. Most horses tend to land with the lateral heel first at walk (Wilson et al. 2016). The impact phase can be divided into primary impact phase and secondary impact phase, as seen in **Figure 11 A and B**. Primary impact phase is the first contact between the hoof and the ground. The hoof is colliding with the surface, and absorbing forces, causing impact vibrations and deceleration of the hoof. The vertical forces on the hoof are low at this stage (Gustås et al. 2001; Oosterlinck et al. 2017). The secondary impact phase, **Figure 11 B**, represents the beginning of the collision of the body with the leg, meaning that the forces and vibrations are transmitted to more proximal structures. The vertical forces are increasing, while the hoof decelerates horizontally until it is firmly planted in the surface. Some degree of sliding is normal in this phase (Gustås et al. 2001; Oosterlinck et al. 2017).

The impact phase is followed by the support phase, **Figure 11 C**. It makes up most of the collision of the body with the leg, as the deceleration of the hoof has ceased. During the

support phase, the vertical force reaches its maximum. Studies have shown that the vertical force maximum at medium trot is approximately 1.2 times the horse's bodyweight (Merkens et al. 1993), and at fast gallop possibly up to 2.5 times the horse's bodyweight (Witte, Knill, and Wilson 2004). After the support phase, the breakover follows, **Figure 11 D**, which is the part where the hoof accelerates again to leave the ground. The heel of the hoof starts to leave the ground by a forward rotation, causing the vertical forces to gradually decrease towards zero. When the hoof rolls off the ground, the swing phase starts.

The swing phase is initiated by the post-breakover. This is the period immediately after the hoof loses contact with the ground and includes the rotation of the hoof mid-air. The hoof stays in mid-phase until it enters pre-impact phase, just before hitting the ground (Thomason and Peterson 2008).
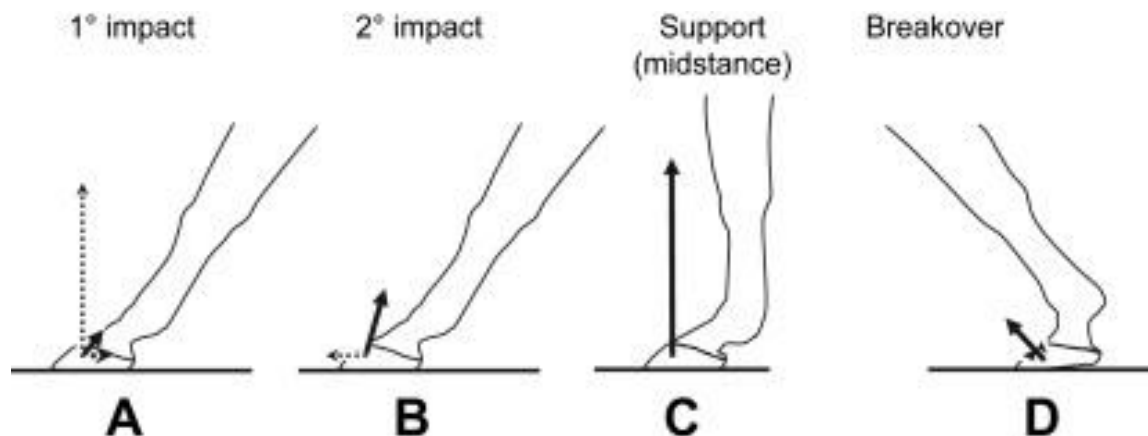


*Figure 11: The different phases of the stance phase. Phase A shows the 1st impact, B the 2nd impact, C the midstance and D breakover. Adapted from Thomason & Peterson, 2008.*

### 3.1.3 Hoof biomechanics

The hoof can be divided into three functional areas: the heels for damping, the wall, frog, and sole for support and the toe for propulsion. The hoof undergoes a deformation at stance phase, which allows shock absorption, and dissipation of the forces (Pollitt 1992; Dyhre-Poulsen et al. 1994). The main deformation takes place at the caudal part of the hoof, where the hoof is the most elastic compared to the toe and quarters (Oosterlinck et al. 2017)). At impact, the sole and frog exhibit a downward movement which cause the proximal dorsal hoof wall to move back, and the quarters to flare to the side, causing a heel expansion (Hinterhofer et al. 2006; Colles 1989; Kai et al. 2000; Douglas et al. 1998) as illustrated in **Figure 12.** The heel expansion is at its widest at impact. Correspondingly, the distance between the heels is at its narrowest at breakover, due to the increased pressure at the toe. The deformation of the hoof during stance phase optimises the functional areas of the hoof and is considered important for blood perfusion of the hoof and distal limb (Yoshihara et al. 2010).
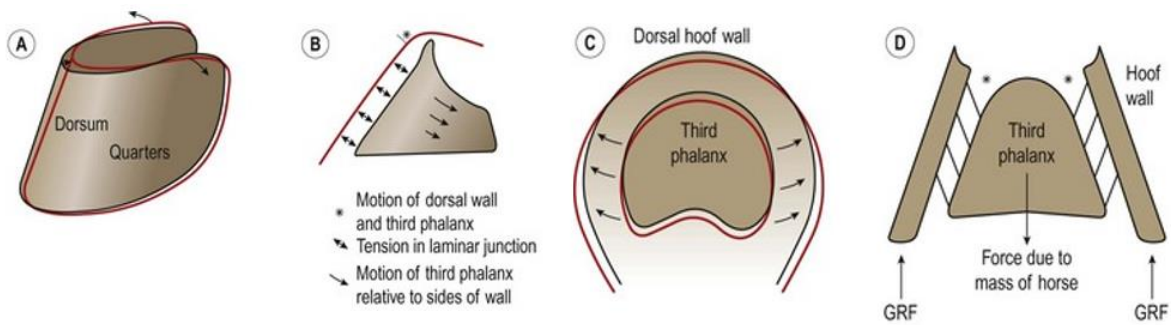
*Figure 12: The hoof mechanism. Adapted from Douglas et al., 1998.*

## 3.2 Hoof management

"No foot, no horse" is a well-known saying among equestrians, which emphasises the significant role of hoof care for both equine welfare and performance (Davies et al., 2002; Reilly et al., 1995). Proper farriery promotes a healthy functional foot and biomechanical efficiency and prevents lameness. This section will provide an introduction of the importance of trimming and the possibility of shoeing a horse.

### 3.2.1 Trimming

The hoof is a three-dimensional structure, and the balance of the hoof is reckoned to contribute to the overall balance of the horse as it ensures an optimal distribution of forces during locomotion (Balch et al., 1997; Davies et al., 2002). A routine trimming of the hooves consists of maintaining a straight hoof axis, trimming the hoof wall as needed, and conserving the frog (Hood et al., 2001; O'Grady and Poupard 2003).

Hoof balance is traditionally evaluated by a visual assessment of the hoof by a static and dynamic evaluation. Trimming for static hoof balance strives for a geometric equilibrium of the limb and hoof, when the horse is standing in a square position. Trimming aims for symmetry of the hoof, with equal lengths of the medial and lateral hoof wall, in addition, the axis of the limb should be perpendicular to the ground surface (van Heel et al. 2004; O'Grady and Poupard 2003).

Dynamic balance is evaluated in motion and strives for the hoof-conformation allowing the hoof to contact the surface in a prescribed pattern (Hood et al., 2001; O'Grady and Poupard 2003). Trimming for symmetry indicates that a flat-footed landing would be expected. However, research has shown that most horses tend to land with the lateral heel first, in both front and hind hooves, which is not altered by a trimming striving for symmetry and furthermore not distinguishable from flat-foot landing by a visual evaluation (Back et al., 2013). The limitations of the human eye lie in the temporal resolution of 24hz, which means that humans can detect events that are <40ms apart. The landing pattern of the hoof is normally shorter than 40ms and thus not detectable to the eye. A clearly visible landing pattern, for example toe first, is abnormal and implies that there is an underlying problem, or the hoof is in imbalance(van Heel et al. 2004). A correct trimming is of fundamental importance before any horseshoe is applied. (Parks 2011b; Oosterlinck et al. 2017).

### 3.2.2 Horseshoes

Hoof growth is in most cases not able to keep up with the excessive wearing of the hooves caused by hoof-ground friction, which can cause imbalance of the hoof (Hood et al., 2001). The primary reason for applying horseshoes is therefore to protect the hooves from excessive wear (Roepstorff, Johnston, and Drevemo 1999). The current techniques of shoeing a horse are still like those developed centuries ago, regardless of the purpose of the shoe (van Heel et al. 2005). Farriery techniques still rely on empiric, traditional expertise rather than scientific evidence (Weller et al. 2018). Trimming and shoeing should aim for biomechanical efficiency, promote a healthy functional foot, prevent lameness, and may also be useful in the treatment of a pre-existing pathology (Oosterlinck et al. 2017; O'Grady and Poupard 2003).

Shoeing a horse with a standard steel shoe elevates the hoof from the ground and affects the hoof mechanism by allowing less expansion of the hoof wall compared to an unshod horse (Roepstorff et al., 2001a). The contraction of the wall at the heel during late stages of stance phase, is also attenuated by shoeing ((Roepstorff et al., 2001b). Without a shoe, the hoof wall compression at the quarters and toe remains more constant and less in magnitude, than with a shoe. In a shod horse, friction between the expanding heel of the hoof and the horseshoe cause greater wear of the heel than the toe of the hoof. Over time, this wearing will cause imbalance, making it necessary to regularly remove the shoe, trim the hoof and reapply a new shoe(van Heel et al. 2004; Moleman et al. 2006). However, an optimal trimming/shoeing interval is not yet scientifically defined, as the research on routing farriery is scarce (Weller et al. 2018). Moleman et al., 2006 suggested that such an interval should be determined for each individual horse, to meet its needs. The length of the recommended shoeing interval within research varies between 4-6 weeks, or 6-8 weeks (van Heel et al. 2005; Moleman et al. 2006; Leśniak et al. 2017). Anecdotally, common shoeing/trimming intervals consist of 4 to 8 weeks. The interval might be influenced by the financial situation of the horse owner, and their knowledge and understanding of equine hoof care.

Attaching a horseshoe to a hoof is usually done by nailing the horseshoe to the hoof with nails. However, gluing the shoe to the hoof is also possible and can be used in cases with a thin or poor hoof wall (Yoshihara et al. 2010). The placement of the nails in the hoof can limit the hoof mechanism, especially regarding heel expansion. Making sure the nails are not fastened too close to the heel and fitting the shoe slightly wider than the hoof in the heel area, minimises the limiting effect horseshoes has on the hoof mechanism (O'Grady et al., 2017). Yoshihara et al., 2010 showed that the gluing of horseshoes does not limit the heel expansion in the front hooves, compared to nailing an steel shoe. However, in the same study, heel contraction at breakover was significant more limited by gluing a horseshoe to the hoof compared to nailing, both at the front and hind hooves.

### 3.3 Equine locomotion biomechanics

Biomechanics is the study of the function and structure of biological systems, such as the movement of animals by means of the methods of mechanics. The main principles of equine locomotion biomechanics, in connection with quantitative gait analysis, will be described in the following section.

### 3.3.1 Relevant planes and anatomical positions

Locomotion involves rotation and translation of the equine body segments, regardless of the gait performed. The horse's body rotates and translates in three dimensions, that can be

described using a global coordinate system. The global coordinate system consists of three two-dimensional planes called the sagittal, dorsal, and transverse planes, and the three axes of rotation known as the vertical, longitudinal, and transverse axes, as shown in **Figure 13.** Movements of the equine body segments can be described relative to these planes and axes (Clayton et al., 2017).
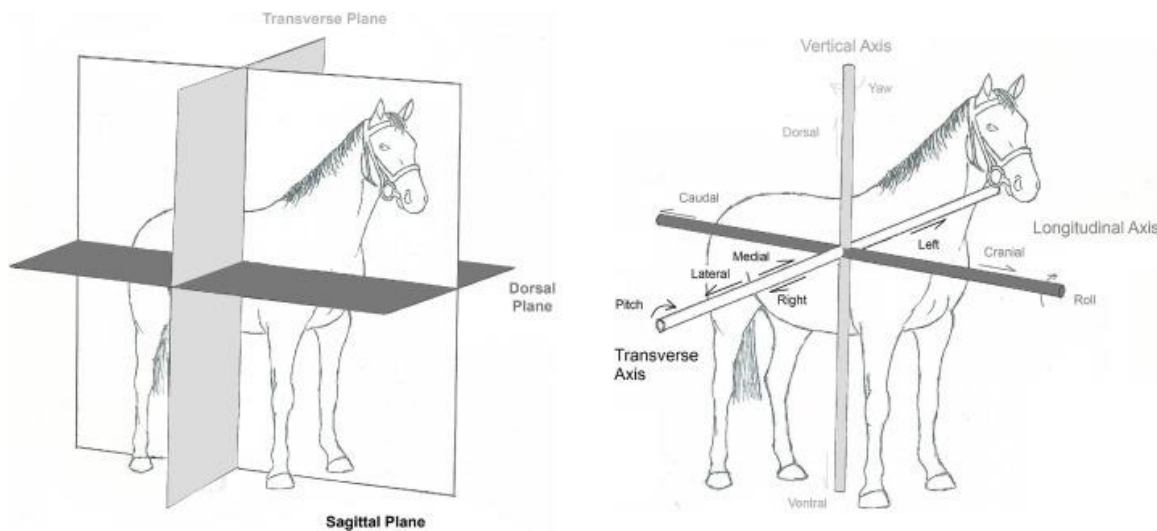


*Figure 13: Equine planes and rotation. Adapted from Bosch et al., 2018.*

A variety of sensors can be positioned on several relevant anatomic landmarks as shown in **Figure 14.** For hoof related parameters, a measurement unit can be mounted onto the hoof wall. For example, either on the dorsal surface as in the research of Moore et al., 2019, or on the lateral hoof wall as in the research of Back et al., 2006.
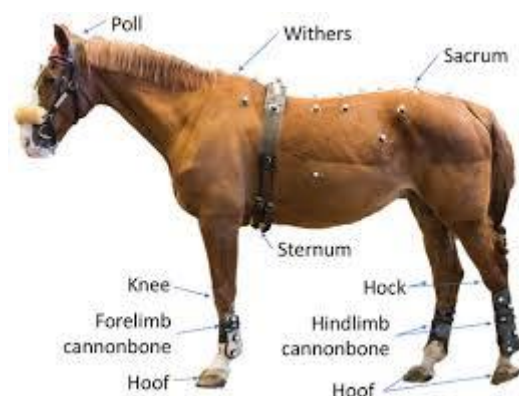


*Figure 14: Relevant positions of sensors used for quantitative gait analysis. Adapted from Bosch et al., 2018.*

### 3.3.3 Quantitative gait analysis

The traditional way of evaluating a horse's locomotion pattern is to let the horse undergo a subjective locomotion assessment by an experienced clinician (Kuiper et al., 2016). There are several contexts where an orthopaedic evaluation of the horse is desired, lameness examination; furthermore, as a key component of the pre-purchase examination, fit-to-compete evaluation at a competition, or as a part of stallion- or mare-selection for breeding purposes. The subjective evaluation is based on a visible alteration of the gait, other than the natural gait pattern. Most subjective gait evaluations include an evaluation of walk and trot on straight line, and on circle, on both hard and soft surfaces (Kuiper et al., 2016). In some contexts, flexion tests and/or diagnostic anaesthesia are included in the gait evaluation (Kuiper et al., 2016). Subjective locomotion assessment has some shortcomings (Keegan et al., 2007) due to the limitation of the human visual symmetry perception (Parkes et al. 2009) and the bias effect, when interpretating a nerve block (Arkell et al. 2006). Scientific studies have shown high inter-rater variation when assessing lameness both during trot on straight line (Keegan et al. 2010), and during lunging on circles (Hammarberg et al. 2016), this can lead to discussion and poor agreement between clinicians. To overcome these shortcomings, the development of objective locomotion assessment has been encouraged within equine research the last decades.

Quantitative gait analysis has potential to become a complementary, and eventually indispensable tool to improve equine locomotion evaluation, providing objective and unbiased information (Bosch et al. 2018; Serra Bragança et al., 2018). The development of objective locomotion assessment provides scientific evidence for technical solutions that can be used for veterinarians and researchers and improve the communication between veterinarians and towards clients (Keegan et al., 2007). The new quantitative gait analysis technologies and measurements tools make it possible to quantify the effects of farriering and different horseshoes on equine locomotion, for equine professionals including farriers, veterinarians, and researchers. The development of more accessible and reliable quantitative gait analysis tools has started the emergence of evidence-based farriery, which still needs development (Weller et al. 2018).

### 3.3.4 Kinetics and kinematics

Quantitative gait analysis can be divided into two large subgroups: kinetics and kinematics. Kinetics is the study of the forces associated with movement, while kinematics is the study of motion of body segments (Buchner et al., 2010; Chateau et al., 2009a; Oosterlinck et al., 2010a; Weishaupt et al., 2002). Kinetics are not within the scope of this paper, therefore only a short description of kinetics will be given.

**Kinetics**

Kinetic methods measure the forces associated with locomotion. In horses these forces are present at the hoof-ground-interaction. The ground-reaction force applied from the ground to the limb during the stance phase can be divided into three components: in the vertical direction (Fz), in the craniocaudal direction (Fy) and in the mediolateral direction (Fx) as illustrated in **Figure 15** (Oosterlinck et al. 2017).
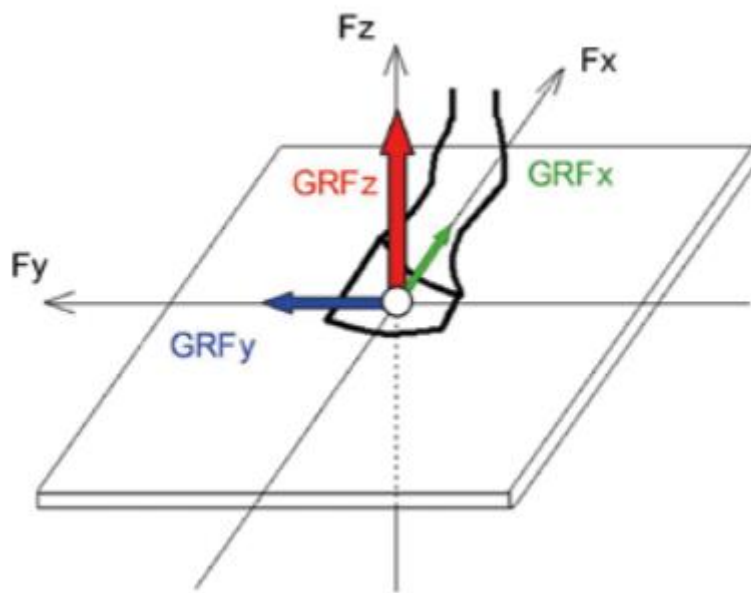
*Figure 15: Forces at hoof-ground interaction. The ground reaction force (GRF) is subdivided into Fx, Fy and Fz. Adapted from Osterlinck et al., 2017*

One of the most used tools for kinetics measurements is the force plate. However, a force plate usually is only available in a laboratory environment as the force plate needs to be mounted in a concrete foundation. In addition, retrieving kinetics data from a force plate can be very time consuming as the horse needs to run over the plate several times, hitting the plate with exactly one limb, to get enough acceptable measurements (Merkens et al. 1993). Other possibilities for measuring kinetic parameters are pressure plates (Back et al., 2013), horseshoes with force measuring devices (Kai et al. 2000), or force measuring treadmills (Weishaupt et al. 2002).

**Kinematics**

Kinematic methods analyse the movement of body segments during locomotion, with outputs like stride length and durations, limbs protraction/retraction angles, different ranges of motion, and hoof impact vibration parameters. There are several tools available to measure kinematics. Kinematic measurements nowadays are mostly obtained using Optical Motion Capture (OMC) systems (Guerra-Filho 2005) or Inertial Measurement Units (IMU) systems (Moorman et al., 2012).

*Optical motion capture*

Reflective markers, strategically placed at classical anatomical landmarks on the horse, are used by an OMC system to assess kinematic parameters. Several (infra-red) cameras placed around the examination location track the three-dimensional (3D) position of the markers. The average position error is usually lower than a few millimetres, which makes these systems highly accurate (Eichelberger et al. 2016; Windolf et al., 2008) and therefore the golden standard for kinematic analysis (Bolink et al., 2016). However, a significant number of OMC cameras and supporting infrastructure is needed for a full body capture of equine locomotion, which is connected to high costs and usually only obtained in a fixed laboratory setting or large clinics (Bolink et al. 2016).

34

*Inertial measurement unit*

Inertial measurement unit systems are based on wireless sensors, instead of markers as with OMC (Bosch et al. 2018; Keegan et al. 2010; Pfau et al., 2005). There is a set of 3D measuring components in the IMU including accelerometers, gyroscopes, magnetometers, and sometimes a GPS, which together make it possible to measure kinematic parameters (Pfau et al., 2005). The IMU sensors are small, portable, and in contrast to OMC, can be adapted to a field setting for equine veterinarians and researchers.

EquiMoves® system makes use of wireless IMU-based sensors, developed for equine application purposes (Bosch et al. 2018). The IMU's are attached to relevant anatomical landmarks on the horse, and the displacement, of that landmark can be measured. EquiMoves® system usually makes use of a sampling frequency of 200Hz, which is considered sufficient for equine gait analysis (Bosch et al. 2018). For measurements which require a higher sampling frequency, such as hoof impact vibrations, the EquiMoves®, sensors can be set to a sampling frequency of 1000 Hz.